Full length article

Mechanistic insights into the generation and control of Cl-DBPs during wastewater sludge chlorination disinfection process

Weijun Zhang [a,b], Tianyi Dong [a,b], Jing Ai [a,b,*], Qinglong Fu [a,b], Nan Zhang [a,b], Hang He [a,b], Qilin Wang [d], Dongsheng Wang [b,c]

[a] Hubei Key Laboratory of Yangtze Catchment Environmental Aquatic Science, School of Environmental Studies, China University of Geosciences, Wuhan 430074, Hubei, China
[b] State Environmental Protection Key Laboratory of Source Apportionment and Control of Aquatic Pollution, Ministry of Ecology and Environment, Wuhan 430074, Hubei, China
[c] Department of Environmental Engineering, Zhejiang University, Hangzhou 310058, Zhejiang, China
[d] Centre for Technology in Water and Wastewater, School of Civil and Environmental Engineering, University of Technology Sydney, Sydney, NSW 2007, Australia

ABSTRACT

Chlorination disinfection has been widely used to kill the pathogenic microorganisms in wastewater sludge during the special Covid-19 period, but sludge chlorination might cause the generation of harmful disinfection byproducts (DBPs). In this work, the transformation of extracellular polymeric substance (EPS) and mechanisms of Cl-DBPs generation during sludge disinfection by sodium hypochlorite (NaClO) were investigated using multispectral analysis in combination with Fourier transform ion cyclotron resonance mass spectrometry (FTICR-MS). The microorganism *Escherichia coli* (*E. coli*) was effectively inactivated by active chlorine generated from NaClO. However, a high diversity of Cl-DBPs were produced with the addition of NaClO into sludge, causing the increase of acute toxicity on Q67 luminous bacteria of chlorinated EPS. A variety of N-containing molecular formulas were produced after chlorination, but N-containing DBPs were not detected, which might be the indicative of the dissociation of $-NH_2$ groups after Cl-DBPs generated. Additionally, the release of N-containing compounds was increased in alkaline environment caused by NaClO addition, resulted in more Cl-DBPs generation via nucleophilic substitutions. Whereas, less N-compounds and Cl-DBPs were detected after EPS chlorination under acidic environment, leading to lower cell cytotoxicity. Therefore, N-containing compounds of lignin derivatives in sludge were the major Cl-DBPs precursors, and acidic environment could control the release of N-compounds by eliminating the dissociation of functional groups in lignin derivatives, consequently reducing the generation and cytotoxicity of Cl-DBPs. This study highlights the importance to control the alkalinity of sludge to reduce Cl-DBPs generation prior to chlorination disinfection process, and ensure the safety of subsequential disposal for wastewater sludge.

1. Introduction

At the end of 2019, the COVID-19 respiratory pandemic caused more than 350 million confirmed cases in 216 countries (until January 20th, 2022) with a fatality rate of 3.3% (WHO, 2020). Person-to-person transmission is the primary means of the spread for severe acute respiratory syndrome coronavirus 2 (SARS-CoV-2), the agent causing COVID-19, which occurs via direct contact or indirect spread of droplets by an infected individual coughing or/ and sneezing (Rothan et al., 2020), or through microdroplets spread during loud conversations and breathing

(Ningthoujam et al., 2020; Carrillo-Reyes et al., 2021). During this special period, the sludge produced from wastewater treatment plant (WWTP) contains plenty of extracellular polymeric substance (EPS) that provides suitable conditions to viral transmission like enteroviruses (Chen et al., 2014; Wang et al., 2020), hepatitis A virus (Prado et al., 2012) and papillomavirus (Bibby et al., 2013) and such all. Thus, the COVID-19 viruses are also possible to infect humans via indirect contact during sludge management, transportation or land-application without proper pre-disinfection treatment. Thereinto, chlorination is one of the most commonly used disinfection in wastewater treatment processes

and simple way to kill various viruses (Chen et al., 2014; Lizasoain et al., 2018; Ma et al., 2010). Thus, chlorination disinfection for killing the viruses in sludge attracted extensive attentions due to the rapid spread of Covid-19, especially for the medical wastewater sludge treatment in the emergency (Yu et al., 2013). However, some remaining negative impacts are also caused by chlorination disinfection to sludge, especially for the disinfection by-products (DBPs) generation, which pose great threats to the eco-environment (Emmanuel et al., 2004). It is of great engineering and scientific importance to investigate the generations and compositions of DBPs during chlorination disinfection processes so as to establish a safe and effective sludge disinfection approach.

The first U.S. Environmental Protection Agency (EPA) regulation pronounced that chloroform and other DBPs could cause adverse toxic impacts on the eco-environment in 1979, and regulations on DBPs were expanded after 1998 (EPA, 2006). During the last few decades, dissolved organic matter (DOM) was reported to be important DBPs precursors, and numerous studies focused on linking specific DBPs to DOM (Zhang et al., 2002). However, the wastewater sludge contained plenty of organic matters (especially EPS) that were also closely associated with the generation of DBPs during chlorination disinfection process (Xiao et al., 2018). The generated DBPs remained in sludge after disinfection could cause severe toxicity impacts on the eco-environment in the subsequential land application (Fytili et al. 2008), landfill (Gude et al., 2015) and agricultural fertilizer (Praspaliauskas et al., 2017). Thereinto, concerns on public health spurred the identification of unknown DBPs and their precursors to optimize sludge chlorination disinfection processes for minishing the exposure to toxic chemicals was lightened (Richardson et al., 2018). As primary precursor, EPS in sludge composed of extremely complex organic matters from microorganisms and possessed plentiful phenols or polyphenolics (e.g. lipids, lignin, tannins, etc.) (Liu et al., 2020; Zhao et al., 2017), which can react with chlorine to form toxic halophenols (Pan et al., 2013), halo-benzoquinones (Zhai et al., 2014), haloketones (Kristiana et al., 2009), trihalomethane (THMs) (Qin et al., 2010), and other halogenated analogues. Nevertheless, the diverse organic molecules in sludge might result in the generation of DBPs with great varieties under chlorination, but current knowledge is still limited due to the poor consciousness upon sludge chlorination disinfection process.

In addition, it still remains uncertain that what kind of DBPs can be formed from EPS derived from sludge, and the characterization of unknown DBPs in sludge is also a great challenge. The formation of uncharacterized DBPs is a public health concern, and even some DBPs in sludge are more toxic than the organic pollutants in the original waste sludge (Gao et al., 2020). However, the relationship between disinfectants and toxic DBPs during sludge disinfection has not been explored. Recently, carbonyl DBPs have been paid extension attentions due to their cytotoxicity and carcinogenicity (Li et al., 2018; Prasse et al., 2018; Richardson et al., 1999), that made significant contributions to the DBPs associated toxicity on the eco-environment, in which carbonyl-EPS derived from sludge probably contributes significantly to the precursors that form known DBPs. Additionally, the formation of N-DBPs and N-free-DBPs arising from chlorination has been also reported and in particular the formation of organic chloramines (Zhang et al., 2016) in water environment. Aromatic structure in organics is easier to generate Cl-DBPs via electrophilic substitution or addition by halogens during chlorination disinfection (Tomlinson et al., 2016). The primary component EPS in sludge contains abundant carbonyl and aromatic structures, as well as N-containing compounds, that were all probably form harmful Cl-DBPs. Therefore, it is of great importance to develop more accurate method for DBPs characterization in waste sludge, and control the chlorination operating conditions for reducing DBPs generation during sludge disinfection processes.

These few decades, the DBPs with more complex structures were detected due to rapid improvement of mass spectrometry (MS) with highly sensitivity and resolution. For instance, trihalo-HCDs (i.e., 2,2,4-trihalo-5-hydroxy-4-cyclopentene-1,3-diones) and its homologous compound of trihalo-HCD (i.e., 2,2,4-trichloro-5-methoxycyclopent-4-ene-1,3-dione) were observed during chlorination disinfection to drinking water (Zhai et al., 2014; Pan et al., 2016 or syringaldehyde (Gong et al., 2005). In addition, Gonsior (2019) also found lots of unknown DBPs that generated from disinfection of dissolved organic matters (DOM) in lysed *Microcystis aeruginosa* cells, via negative mode electrospray ionization Fourier transform ion cyclotron resonance mass spectrometry (ESI FT-ICR-MS). This approach was reported to be capable of determining the exacted molecular formulas of DBPs (Gonsior et al. 2009/ 2014; Lavonen et al., 2013), which may be directly related to DOM sources in wastewater or drinking water. However, there were no studies have been reported related to the DBPs generation during sludge disinfections. The unknown DBPs can be also formed during sludge chlorination disinfection process, the composition and structural characterizations of formed-DBPs during chlorination disinfection process is of great importance to elucidate the DBPs generation route, and prevent the DBPs generation to reduce their cytotoxicity. However, there is limited information upon the types and composition of DBPs during sludge chlorination disinfection, as well as their potential negative impacts on the eco-environment has not been concerned.

To fill these knowledge gaps in the sludge chlorination disinfection process, the objectives of this study were to (i) optimize the sludge chlorination disinfection conditions by evaluating the microorganism *Escherichia coli* (*E. coli*) activities and their acute cytotoxicity on Q67 luminous bacteria; (ii) investigate the structural compositions of EPS and Cl-DBPs in sludge using negative mode electrospray ionization Fourier transform ion cyclotron resonance mass spectrometry (FTICR-MS) in combination with ultrahigh resolution mass spectrometry (MS^2); (iii) explore the relationships between EPS transformation and Cl-DBPs generation mechanisms during sludge chlorination disinfection process, and elucidate the major precursor compositions in EPS for Cl-DBPs generation. The results of the study could provide significance scientific guidance for Cl-DBPs generation control in sludge chlorination disinfection fields.

2. Materials and methods

2.1. Sludge properties

Waste activated sludge (WAS) was collected from a municipal wastewater treatment plant (WWTP) located in Beijing, China. The ratio of volatile suspended solids to total suspended solids (VSS/TSS) in the sludge sample was 55.7%, that was determined according to procedure described by Cai (2018). Other detailed information for WAS was provided in **Supporting Information** (**SI**) **Table S1**.

2.2. Chemicals and materials

Details for chemicals and materials used in this study were described in **SI Text S1**.

2.3. Procedure for sludge chlorination disinfection

The batch experiments for chlorination disinfection of sludge were performed in flask beakers (1 L) under stirring by a hexagonal agitator (MY3000-6B). First, 300 mL of raw WAS was transferred into 1-L flask beakers, then disinfected by sodium hypochlorite (NaClO) through the following procedure: adding NaClO with 2 min of rapid mixing (250 rmp), followed by slowing mixing (150 rmp). The doses of NaClO were set as 0, 25, 30, 32, 34, 36, 40 mg/g per total suspended solids (TSS), and the slowing mixing time is controlled by 360 min. In addition, the same mixing procedure was applied in the pH adjustment experiment. It should be noted that WAS was adjusted to pH = 2.5 using HCl (0.25 mol/L) prior to NaClO disinfection. After the disinfection process, the sludge sample was withdrawn for pathogen (*E. coli*) concentration and acute toxicity determinations.

2.4. *Escherichia coli activity and acute toxicity tests*

The *Escherichia coli* (*E. coli*) was chosen as the indicator of pathogen concentrations and measured by counting most probable number (MPN) via fermentation method, to evaluate the effectiveness of sludge disinfection by NaClO. Details for *E. coli* activity analysis was provided in **SI Text S2**.

The luminescent bacteria (Vibrio qinghaiensis Q67) were used to test the microorganism toxicity of disinfection by-products (DBPs) following the Q67 kit instructions. Specifically, the lyophilized Vibrio qinghaiensis Q67 powder was pre-equilibrated for 15 min at 25 °C. Then, 0.52 mL of recovery buffer (0.85% NaCl) was added into Q67 kit solution and incubated for 10 min. It should be noted that the pH of each sample was balanced following the Q67 kit instructions. For samples testing, 0.05 mL Q67 resuscitation solution was added into a clean test tube containing 2.0 mL samples, and incubated for 15 min before sending to BHP9514 type drinking water safety fast detector (HAMAMATSU, China) for Q67 luminescence intensity measurement. Meanwhile, the luminescence intensity of Q67 in recovery buffer was used as the negative control blank (100% luminescence). The Q67 luminescence inhibition rate (LIR) represented the degree of toxicity which was calculated according to the following formula:

$$LIR(\%) = \frac{\text{luminrscent value of the recovery buffer} - \text{luminescent value of the samples}}{\text{luminescent vale of the recovery buffer}} \times 100$$

2.5. *Fourier-transform infrared spectroscopy combined with 2D-COS analysis of EPS under chlorination disinfection process*

To investigate the role of EPS in the Cl-DBPs generation during sludge chlorination process, the interaction between purely extracted extracellular polymeric substance (EPS) with NaClO was conducted. Meanwhile, the EPS extraction and analysis procedure was provided in **SI Text S3**. To determine the covariances of major groups in EPS during NaClO treatment, the dosage of NaClO to EPS samples was controlled by 0.2 g/L to 12 g/L TSS. The Fourier-transform infrared spectroscopy (FTIR) of the freeze-dried EPS samples before and after NaClO treatments mixed with KBr (mass ratio of 1:100) was conducted on a Thermo Scientific Nicolet 6700 spectrometer. It should be noted that the dosage of freeze-dried EPS to KBr was controlled in consistency to quantitatively analyze the covariances of major groups in intensity. The FTIR spectra were recorded in range of 400–4000 cm^{-1}. To determine the order of predominant functionals groups transformation in EPS during sludge chlorination disinfection process, the two-dimensional correlation analysis (2D-FTIR) was used to assign the FTIR bands and examine their covariation (Noda and Ozaki, 2004).

2.6. *Solid phase extraction of DBPs formed in sludge chlorination*

Before the examination of the mass spectrometry, all samples collected in sludge are needed to be desalted and treated by an established solid-phase extraction (SPE) procedure (Liu et al., 2020) using the proprietary polymeric Agilent Bond Elut PPL resin. Details for organics and generated Cl-DBPs extraction procedures were described in **SI Text S4**. It should be noted that the highly polar Cl-DBPs are lost during solid phase extraction, thus the presented results are only addressing the extractable and ionizable component of EPS and formed Cl-DBPs in sludge (Gonsior et al., 2019).

2.7. *Ultrahigh resolution mass spectrometry analysis of EPS and DBPs*

The ultrahigh resolution mass spectrometry and Bruker Solarix 15 T Fourier transform ion cyclotron resonance mass spectrometer (FTICR-MS) were used to examine EPS and the probable generated Cl-DBPs upon chlorination disinfection process. Ionization was realized using the negative ion mode electrospray ionization (ESI$^-$), and the spray voltage was set into − 4.0 kV. Moreover, the methanolic EPS samples were diluted with pure methanol (Sigma Aldrich Chromasolv) into at ratio of 1:20 to avoid oversaturation and possible space charge effects during the ion cyclotron resonance trap. The flow rate was set constantly at 120 μL/h, and 300 scans were averaged. Meanwhile, molecular weight was collected at range of 100 ∼ 1600 Da. Besides, the autosampler routine was programmed to wash with 10 mmol/L formic acid between each run to lower the risk of carryover. Mass accuracy was lower than 1.0 part-per-million (ppm) and the molecular formula assignments were based on the following atomic numbers:^{12}C$_{1-50}$, ^{1}H$_{1-50}$, ^{16}O$_{0-50}$, ^{14}N$_{0-5}$, ^{32}S$_{0-3}$ and ^{35}Cl$_{0-5}$ and ^{37}Cl$_{0-5}$ isotopologues. Van Krevelen (1950) or elemental diagrams and a modified Kendrick plot were used to visualize FTICR-MS data (Fu et al., 2022). Additionally, the double-bond equivalent (DBE) parameter was used to visualize the saturation stages of presumed chlorinated products, which is essentially a proxy for the degree of saturated of each annotated molecular formula. The Kendrick mass defect (KMD) (CH$_2$)-number of carbon plots were further applied to visualize the homologous series of detected Cl-DBPs (Yuan et al., 2017) in sludge. In addition, MS^2 spectra was further applied for molecular confirmation of each identified Cl-DBPs, which were monitored using an ultimate 3000 UHPLC-Q Exactive orbitrap MS (Thermo Scientific, US) to achieve relatively pure and abundant fragment ions.

2.8. *Other analysis*

The organic concentration in sludge supernatant was analyzed using a total organic carbon analyzer (TOC, Teledyne Tekmar). The molecular weight distribution of EPS was determined using high performance size exclusion chromatograph (HPSEC), details for HPSEC analysis was provided in **SI Text S5**. The full spectrum of UV for sludge supernatant was examined by a UV–vis spectrophotometer (Shimadzu UV-1900, Japan) to quantify the aromaticity of EPS in sludge, and spectra of UV were recorded in the range of 200–900 nm. In addition, the fluorescence excitation emission matrix (EEM) spectroscopy was used to investigate the major component changes of EPS during sludge chlorination disinfection process. Meanwhile, the parallel factor (PARAFAC) analysis was employed to separate the major component from the EEM fluorescence spectra (Hall et al., 2005) data, in which the EEM data was analyzed with the software Mat Lab 8.6 (MathWorks Inc., USA). It should be noted that all samples were filtrated through 0.45 μm cellulose acetate fiber membrane prior to TOC, UV and EEM measurements.

In addition, the spatial distribution of EPS (including proteins, polysaccharides and nucleic acid) in sludge flocs under the different chlorination conditions was characterized using a confocal laser scanning microscopy (CLSM; Zeiss LSM 510) instrument. Details procedure for sludge sample preparation and analysis was provided in **SI Text S3**.
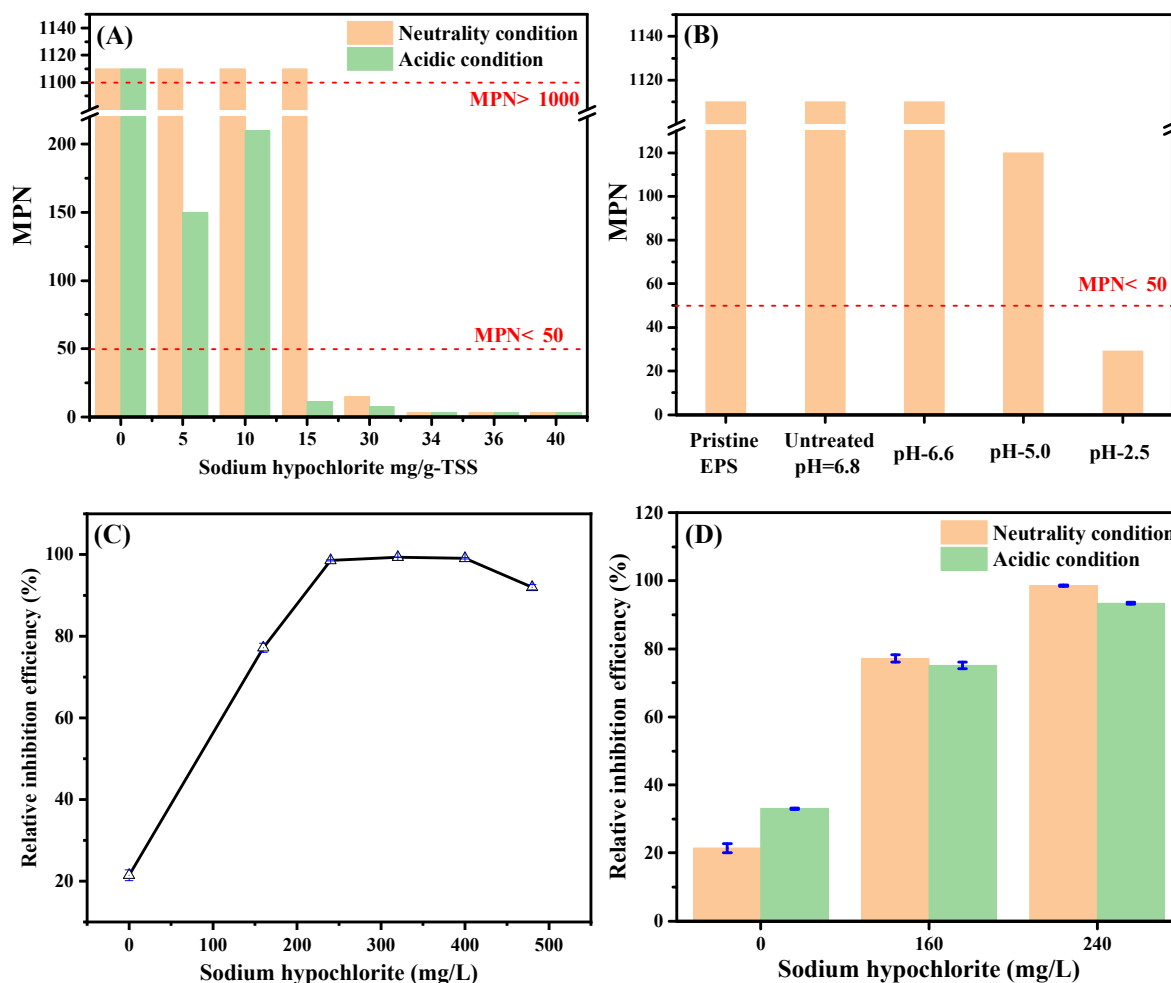
Fig. 1. *E. coli* activities and acute toxicity on Q67 luminous bacteria. (A-B) Effects of NaClO dosage on MPN changes of microorganism *E. coli* in sludge during different chlorination disinfection conditions; (C-D) Effects of NaClO dosage on the relative inhibition efficiency of disinfected EPS on Q67 luminous bacteria. Conditions: NaClO dosage was 15 mg/g-TSS of sludge in (B).

3. Results and discussions

3.1. Effects of NaClO concentration on the E. Coli inactivation

Batch experiments were preformed to evaluate the pathogen microorganism inactivation by NaClO at different pH conditions. As illustrated in Fig. 1A, the pathogen (*E. coli*) was inactivated completely with NaClO dose of 30 mg/g per total suspended solids (mg/g-TSS) of sludge (pH = 8.0) and 15 mg/g-TSS (pH = 2.5), respectively. Besides, when NaClO dosage was 15 mg/g-TSS, the most probable number (MPN) of pathogen (*E. coli*) was lower than 120 at pH < 5.0, and the pathogen (*E. coli*) in sludge was almost inactivated in acidic condition (pH = 2.5) with 15 mg/g-TSS of NaClO. However, 30 mg/g-TSS of NaClO was required to inactivate pathogen (*E. coli*) in sludge when pH > 5.0. These results indicated that the acidic environment significantly enhanced the oxidative ability of NaClO and improve the pathogen inactivation efficiency at lower NaClO dosage.

To get more insights into the role of extracellular polymeric substance (EPS) in the pathogen (*E. coli*) inactivation, the pathogen (*E. coli*) inactivation in purely extracted EPS solution of sludge was also evaluated. The pathogen (*E. coli*) inactivation efficiency in purely extracted EPS solution was consistent with that in sludge environment as shown in Fig. 1B, 300 mg/L (pristine-EPS) and 160 mg/L (EPS pH = 2.5) of NaClO were needed to inactivate the pathogen (*E. coli*). In addition, the cytotoxicity of disinfected by-products (DBPs) on Q67 lumines bacteria was also tested during different sludge chlorination disinfection conditions.

As depicted in Fig. 1C, the relative inhibition efficiency of Q67 lumines bacteria by DBPs increased with NaClO dosage, and the relative inhibition efficiency of Q67 lumines bacteria achieved 100% at 240 mg/L, while 75% at 160 mg/L, indicating the higher cytotoxicity caused at higher dose of NaClO. More specifically, from Fig. 1D, the relative luminescence inhibition efficiency of Q67 bacteria was lower in acidic conditions (pH = 2.5) than that of neutral conditions after EPS was treated by NaClO, suggesting lower acute toxicity of DBPs produced at pH = 2.5 compared to that at pH greater than 5 during sludge chlorination process. Moreover, from **Figures S1**, nucleic acid distribution was also darker after disinfection with NaClO, indicating that the *E. coli.* was effectively inactivated. It should be noted, although the nucleic acid showed higher intensity in pH = 2.5 than that of raw sludge due to the acidolysis, the signal and intensity of nucleic acid was significantly re-reduced after NaClO treatment. These observations indicated that the acidic environment had both advantages for enhancing NaClO oxidation ability and favoring the releasing of nucleic acid from EPS, leading to higher pathogen inactivation efficiency. The Cl-DBPs formed by NaClO treatment under pH = 2.5 exhibited lower toxicity on Q67 luminous bacteria possibly due to less generation of Cl-DBPs. Therefore, the optimal conditions for sludge chlorination disinfection should be 15 mg/g-TSS at pH of 2.5.

3.2. Interaction mechanisms between active chlorine and EPS

3.2.1. EPS transformation during chlorination disinfection process

To investigate the predominant precursor groups of EPS that connected to Cl-DBPs generation and their cytotoxicity during sludge disinfection by NaClO, the three-dimensional excitation-emission matrix (3D-EEM) fluorescence spectroscopy was employed to study the changes of key fluorescence components in EPS by NaClO disinfection in both neutrality and acidic conditions. From **Figure S2**, there was mainly two fluorescence peaks ($E_x/E_m = 230/320$ nm) and ($E_x/E_m = 260/370$ nm) were isolated according to the PARAFAC analysis, associating to tryptophan proteins (TPN) and tyrosine protein-like (TP) components (Chen et al., 2015), respectively. As depicted in **Figure S2**, the two fluorescent intensities decreased significantly after NaClO treatment, indicating the Cl-DBPs generation was mostly associated to these two primary components. Besides, the HPSEC characterization was also applied to examine the average molecular weight (AMW) changes of EPS before and after NaClO treatment. As illustrated in **Figure S3B**, the molecular of 10,580 Da was occurred after NaClO treatment, while there was no 10,580 Da compounds existed after NaClO treatment under acidic (pH = 2.5) condition. There was also no obvious changes in the MW ranged from 600 to 2000 Da in EPS after NaClO treatment at neutral conditions (**Figures S3A and 3C**). However, at acidic conditions (pH = 2.5), the MW of 1232 was degraded into three MWs of 815, 1010, 1020 Da, respectively. The molecular weight loss of these three MWs compounds re-affirmed the

enhanced oxidation ability of NaClO towards EPS in acidic disinfection conditions. Therefore, the distinguishing change features of these compounds were regarded as the possible reasons for different Cl-DBPs generation route under neutrality and acidic chlorination conditions, and TPN/ TP in freely dissolved EPS played a crucial role in Cl-DBPs generation during sludge chlorination disinfection process.

The EPS treated by NaClO was further analyzed using UV spectroscopy to investigate the predominant sites in the aromatic structure of TPN/ TP in Cl-DBPs generation. As depicted in Fig. 2A, zero-order absorbance spectra of EPS exhibited no easily discernible changes caused by the presence of varying concentrations of NaClO. To enhance the spectral resolution, the normalized differential spectra, log-transformed of normalized differential spectra and differential log-transformed spectra were applied to the zero-order absorbance spectra of EPS with various addition of NaClO (Fig. 2**B-D**), respectively. As discussed in **SI Text S6**, all the intensities of the major types of chromophores with peaks at 275, 340 and 395 nm increased consistently with NaClO addition, in which the former one at 275 nm showed greater extent compared to that at 340 nm and 395 nm. In addition, the log-transformed of normalized spectra showed a linear decline with the wavelength, and more regions (e.g., 202–245 nm, 275 nm, > 350 nm) with different slopes were observed, implying there was a heterogeneous distributions of active sites or functional groups on EPS during chlorination disinfection. Moreover, the intensity of the bands/peaks at 223 nm was also enhanced as presented in the derived differential log-
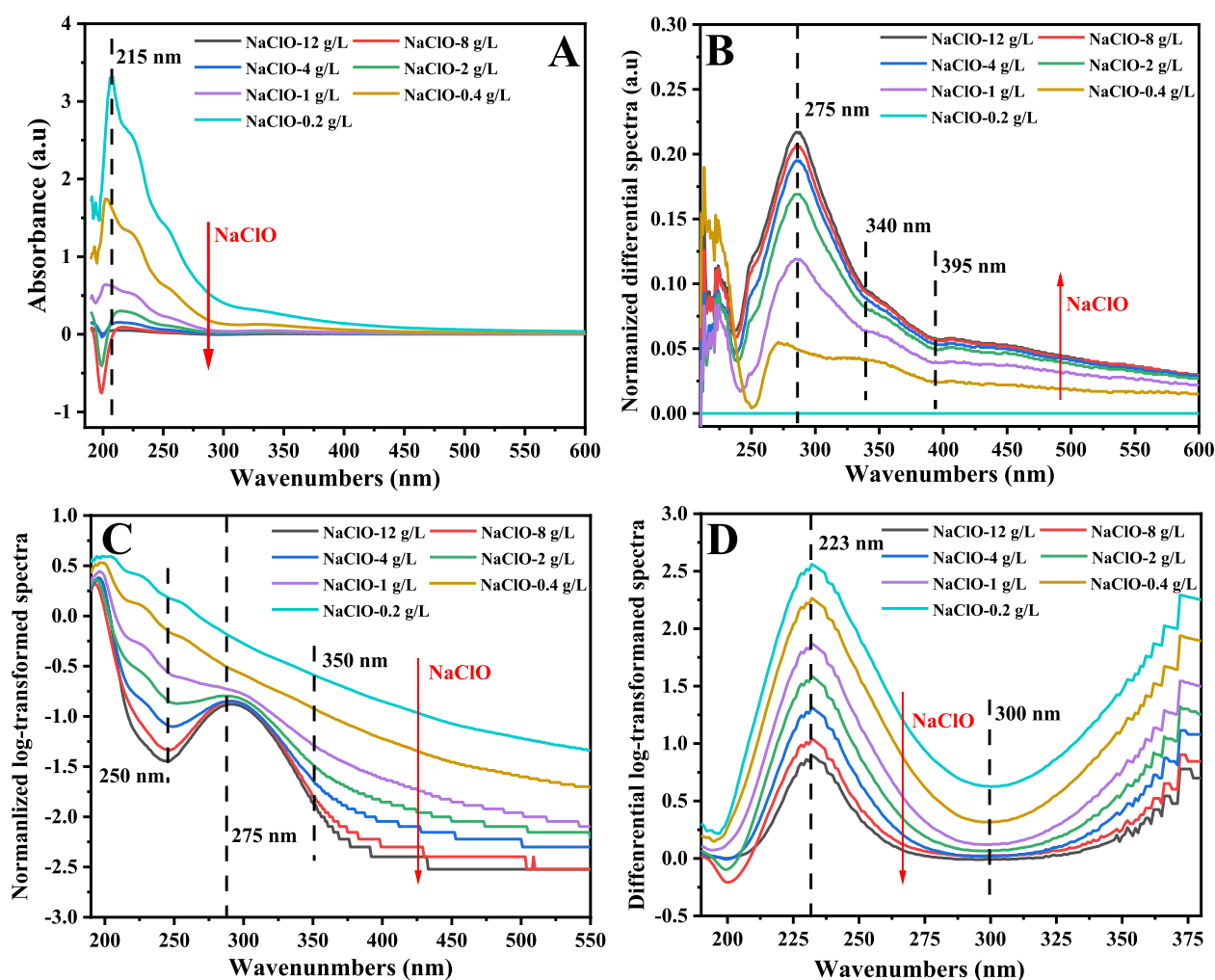

Fig. 2. Changes of zero-absorbance spectra (A), normalized differential spectra (B), normalized log-transformed spectra (C), and differential log-transformed spectra (D) of chlorinated-EPS samples with increasing dose of NaClO. Note: the initial EPS concentration is 247.31 mg/L (TOC). Conditions: the dose of NaClO was controlled by 0.2 g/L to 12 g/L TSS.
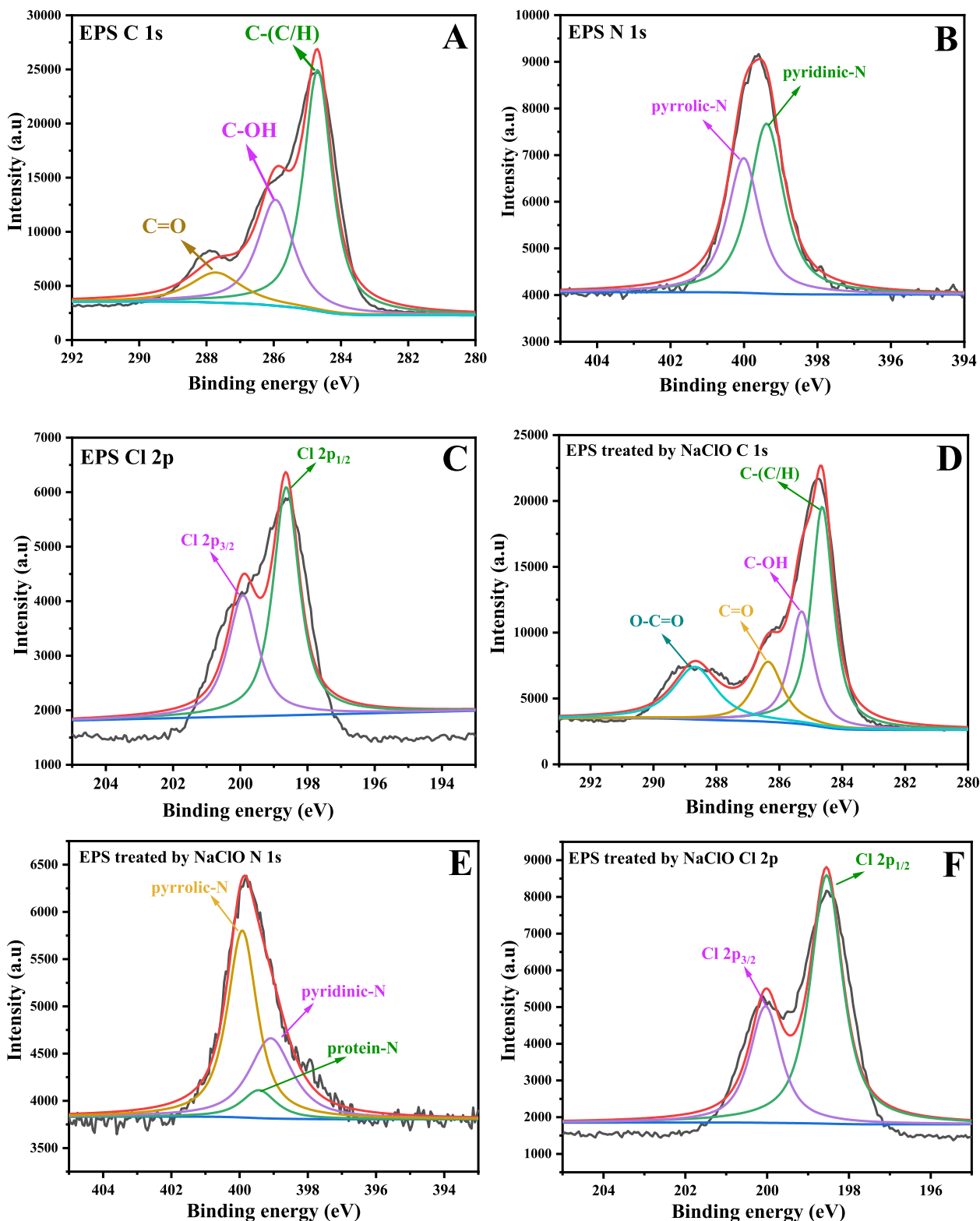
Fig. 3. XPS of EPS in sludge with/without NaClO treatment; (A-C) the C, N and Cl elements spectra of the pristine EPS in sludge; (D-F) the C, N and Cl elements spectra of EPS by NaClO treatment.

transformed spectra of chlorinated-EPS. These results concluded that the addition of NaClO to sludge could induce a slight intensity enhancement for bands/peaks at 223 nm, 275 nm and 300–350 nm, implying the sensitive heterogeneity of these chromophores in EPS were contributed to possible Cl-DBPs generation during chlorination disinfection process.

3.2.2. The contribution of predominant groups in EPS onto DBPs generation

To further characterize the predominant groups transformation in EPS during sludge chlorination, X-ray photoelectron spectroscopy (XPS) investigation was used to analyze the chemical characteristics of the C, N and Cl elements in EPS, and elucidate the contributions of EPS into Cl-DBPs generation during chlorination disinfection. As depicted in

Fig. 3**A and 3D**, the C 1 s signal was resolved into three major component peaks at 284.79, 286.26 and 287.99 eV corresponded to the C-(C, H), C-(O, N) and C = O/O-C-O, respectively, that were commonly found in carboxylic esters, carbonyls, amides or acetals (Ding et al., 2018; He et al., 2020). In the spectra of Cl 1 s (Fig. 3**B and 3F**), the signal of Cl intensity was divided into Cl $2p_{3/2}$ and $2p_{1/2}$, whose intensities were increased significantly, indicating the Cl-compounds generation during the sludge chlorination disinfection process (Hua et al., 2021). In addition, the N 1 s peak appeared at 399.8 eV was correlated to nitrogen in amines or amides (Fig. 3**B and 3E**), which were related to pyrrolic-N, pyridinic-N and protein-N, respectively (Zhu et al., 2016). After 6 hrs of treatment by NaClO, these evidences were completely destroyed, in which the intensities of pyrrolic-N and pyridinic-N decreased from 6800 and 7600 to 4625 and 5500, respectively, indicating that they might be related to fluorescent signatures that were likely to be Cl-DBPs precursors. Besides, the functional groups of EPS structural composition was also characterized using FTIR spectroscopy. An evident increase in peaks at 1490 cm^{-1} assigned to aromatic skeletal C = C vibrations was observed after NaClO treatment, and the intensities of aromatic skeletal C = C vibration increased with dosage of NaClO ranged from 0.04 to 12 g/L-TSS (**Figure S4**). These results revealed that pyrrolic-N, pyridinic-N, protein-N and aromatic compounds in EPS were contributed to Cl-DBPs generation during sludge chlorination.

Although the above results revealed that the pyrrolic-N, pyridinic-N, protein-N and aromatic compounds in EPS were the major Cl-DBPs precursors, but the predominant groups in these compounds contributed to Cl-DBPs generation has not been fully understood. To get more insights of critical groups transformation in EPS during NaClO

disinfection process, the two-dimensional correlation calculation was applied to assign the bands of FTIR spectra (2D-FTIR) and study their covariations. As illustrated in Fig. 4**A-B**, there were two auto-peaks at 1050 and 1460 cm^{-1} presented in the synchronous map of the 2D-FTIR spectra for chlorinated-EPS under neutrality disinfection condition, whereas five predominant auto-peaks at 1760 cm^{-1}, 1640 cm^{-1} (C = O of protein in amid I region), 1480 cm^{-1} (C-O/ COO$^-$ of amino acid), 1100 cm^{-1}, 1000 cm^{-1} (C-OH/ C-O-C of polysaccharides) (Wang et al., 2018; Yin et al., 2015; Xie et al., 2020) were presented in the synchronous map for the chlorinated-EPS under acidic environment (Fig. 4**C-D**), respectively. From the results of **Text S7**, the changes of key components of EPS followed the sequence: C = O of protein in amide I region > C-O/ COO$^-$ of amino acid > C-OH of polysaccharide under neutrality chlorination condition. Whereas, the changes sequence of functional groups followed: C-OH of polysaccharide > C-O/ COO$^-$ of amino acid > C = O of protein in amide I region under acidic environment, which was contrary to that at neutrality condition. It can be concluded the C = O of protein in amide I region showed the fastest transformation under chlorination at neutrality condition that was related to Cl-DBPs generation, while the C-OH of polysaccharide in EPS was more likely to be Cl-DBPs precursors in acidic condition (pH = 2.5). These indicated that the functional groups of both protein C = O and polysaccharide C-OH in EPS played the leading role in the generation of harmful Cl-DBPs.
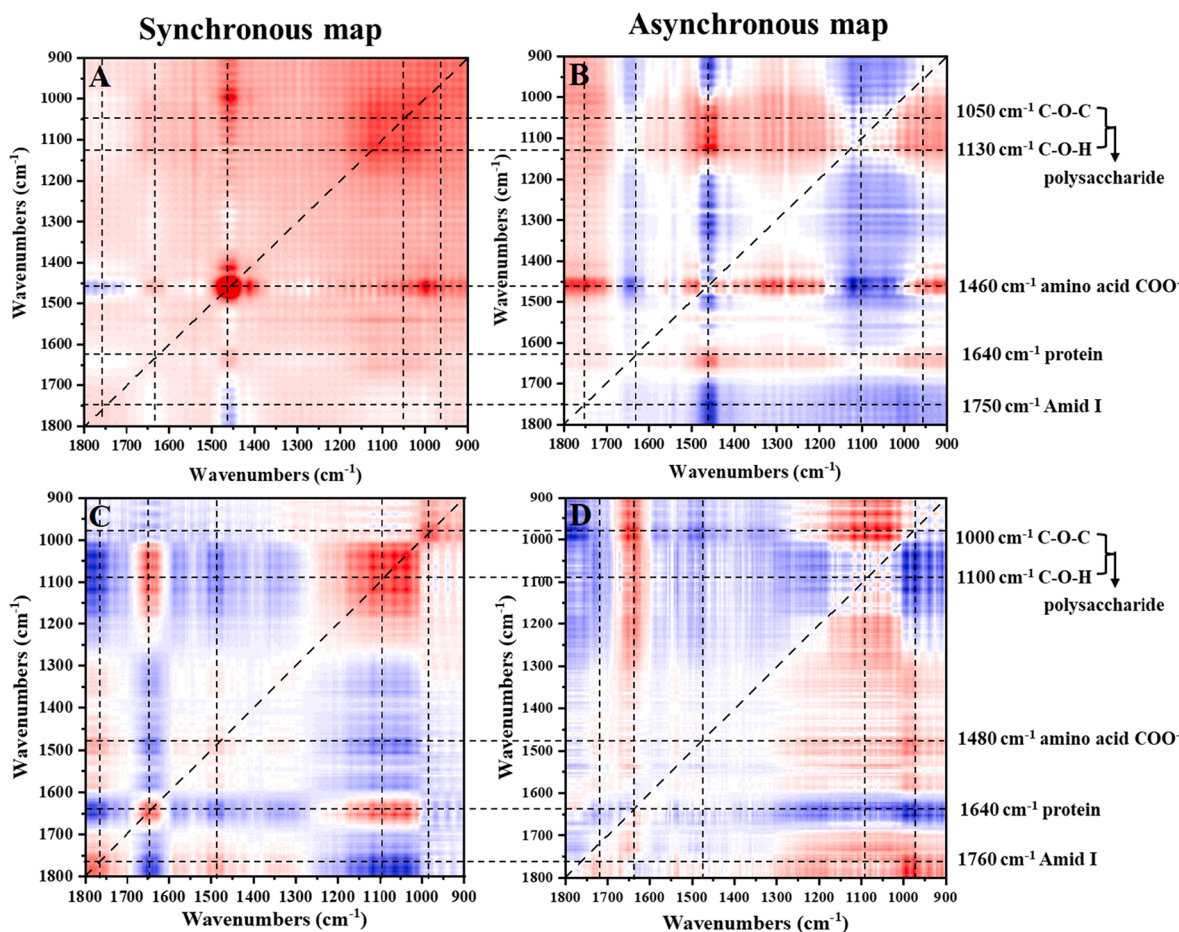

Fig. 4. Synchronous 2D-FTIR-COS (A, C) and asynchronous 2D-FTIR-COS (B, D) of 1800–900 cm^{-1} maps of chlorination disinfected EPS in pH = 6.8 and pH = 2.5, respectively. Red represents positive correlation, and bule represents negative correlation. Higher color intensity indicates a stronger positive or negative correlation. (For interpretation of the references to color in this figure legend, the reader is referred to the web version of this article.)

3.3. Molecular composition of Cl-DBPs during chlorination disinfection process

3.3.1. The molecular characteristics of original organic compounds in EPS

To unravel the mechanisms involved in Cl-DBPs generation during sludge chlorination disinfection, the number and composition of molecules before and after NaClO treatment was further characterized using FTICR-MS. Carbonyl and N-containing compounds in EPS were both important precursors of Cl-DBPs. Here, the Van Krevelen diagram was employed to visualize molecular diversities of EPS component in sludge, and the distribution of detected compounds were further classified by the constructions of H/C and O/C ratio in molecular formulas. In addition, the amount of the possible homologous carbonyl compounds were also presented by the number of points on the horizontal line in KMD (–CH$_2$) diagram. From **Figure 5A, a** large number of molecules with construction of $0.1 \leq O/C < 0.67$ and $0.67 < H/C \leq 1.5$ were observed, that was probably referred to be carbonyl derivates of lignin or carboxylic-rich alicyclic molecule (CRAM) structures (Liu et al., 2020). It should be noted there was significant difference regarding the molecular characteristics between carbonyl derivates of lignin and CRAM structures, in which the CRAM compounds were mainly regarded as aliphatic aldehydes/ketones, but the carbonyl derivates of lignin compounds were more likely to be aromatic aldehydes/ketones structures (Baluha et al., 2013). Besides, amino/carboxyl groups of proteins

and –OH/aldehydes/carbonyl groups of polysaccharide were reported to be abundant as per EPS reference standard, and aromatic aldehydes/ketones could be formed via the interaction by these functional groups, that could also explain the obvious changes in UV absorption at 260–330 nm in EPS by NaClO treatment (seen in Fig. 2). Moreover, a high content of CHOS compounds was also observed, and distributed in lignin and lipid assignment fractions. These S elements were most probably to be present in the form of -SH groups in proteins instead of -SO$_3$ groups in surfactant, as evidenced by no -SO$_3$ losing signal detected in CHOS compounds from the results of the ion collision experiments via MS/MS detection (Figures S5, S6 and S7). However, as depicted in Fig. 6, the distribution of the S-contained molecules before and after the NaClO treatment was not significantly different, indicating that the CHOS compounds in EPS were not the major factor in DBPs cytotoxicity.

Thereinto, detailed composition for carbonyl-CHO compounds was visualized by the oxygen number, and the molecular abundant in numbers was further distinguished by DBE values. As depicted in **Figure 5B-C, a** majority of CHO compounds was distributed in O$_{8-11}$ species with more than 30 molecules, and the O$_{10}$ species possessed the maximum abundant number of 64 molecules. Meanwhile, large amount of O$_{8-11}$ species exhibited high DBE values in the range of 8–13, for instance, both of the molecule series with DBE = 8 for O$_8$ and O$_{11}$ and DBE = 9 for O$_{9-10}$ species contained the maximum number of molecules. These identified CHO molecules in EPS were most probably to be
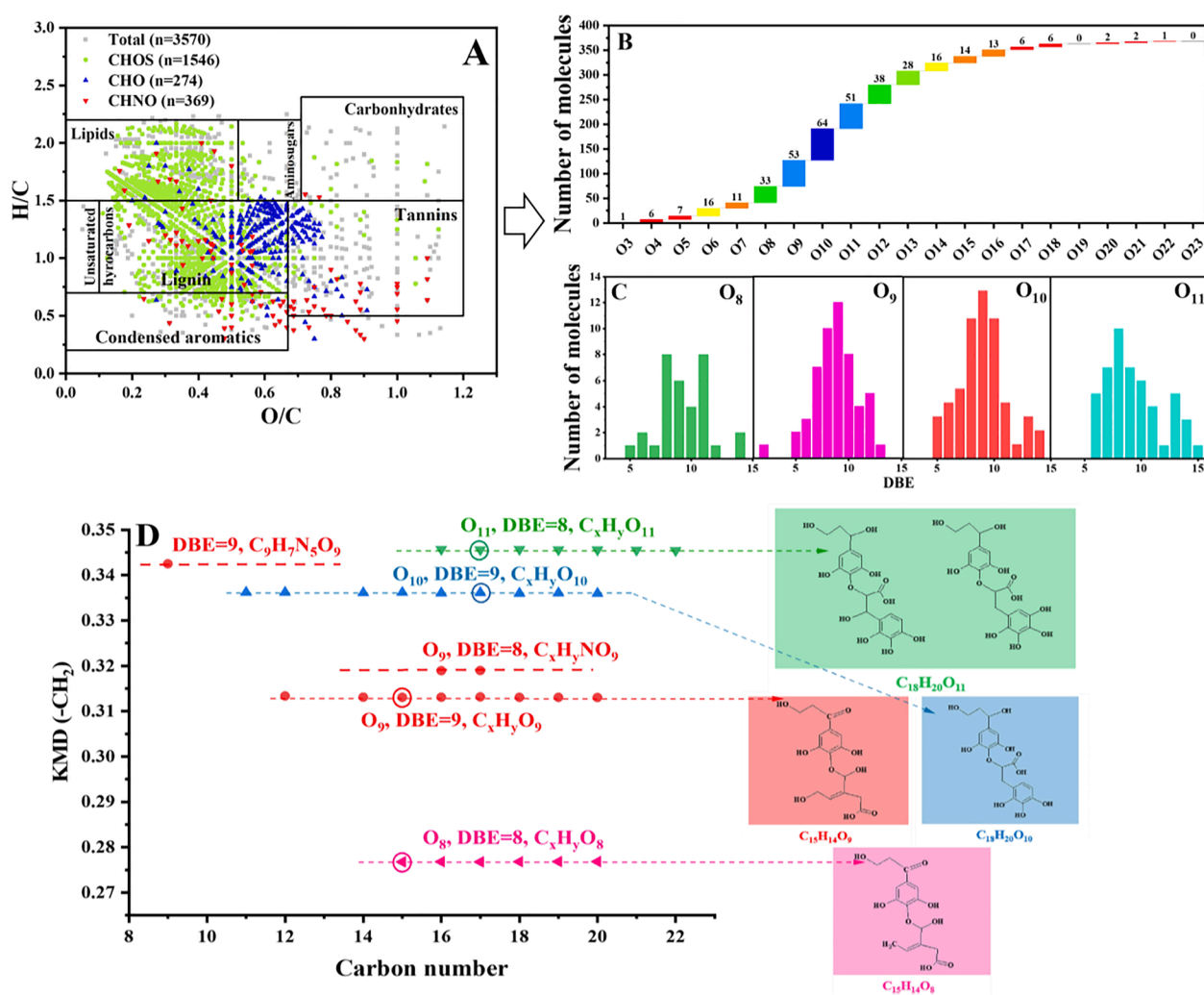

Fig. 5. Molecular characteristics of Cl-DBPs after purely extracted EPS treated by NaClO. (A) Van Krevelen diagrams are based on neutral molecular formula assignments before chlorination disinfection. (B) Composition of chemical formulas contained by the oxygen number; (C) composition of formula compounds in O$_{8-11}$ (EPS) species by DBE values (D) KMD (CH$_2$)-number of carbon plots of formula homologous (S-free) with the proposed structures in pristine-EPS.
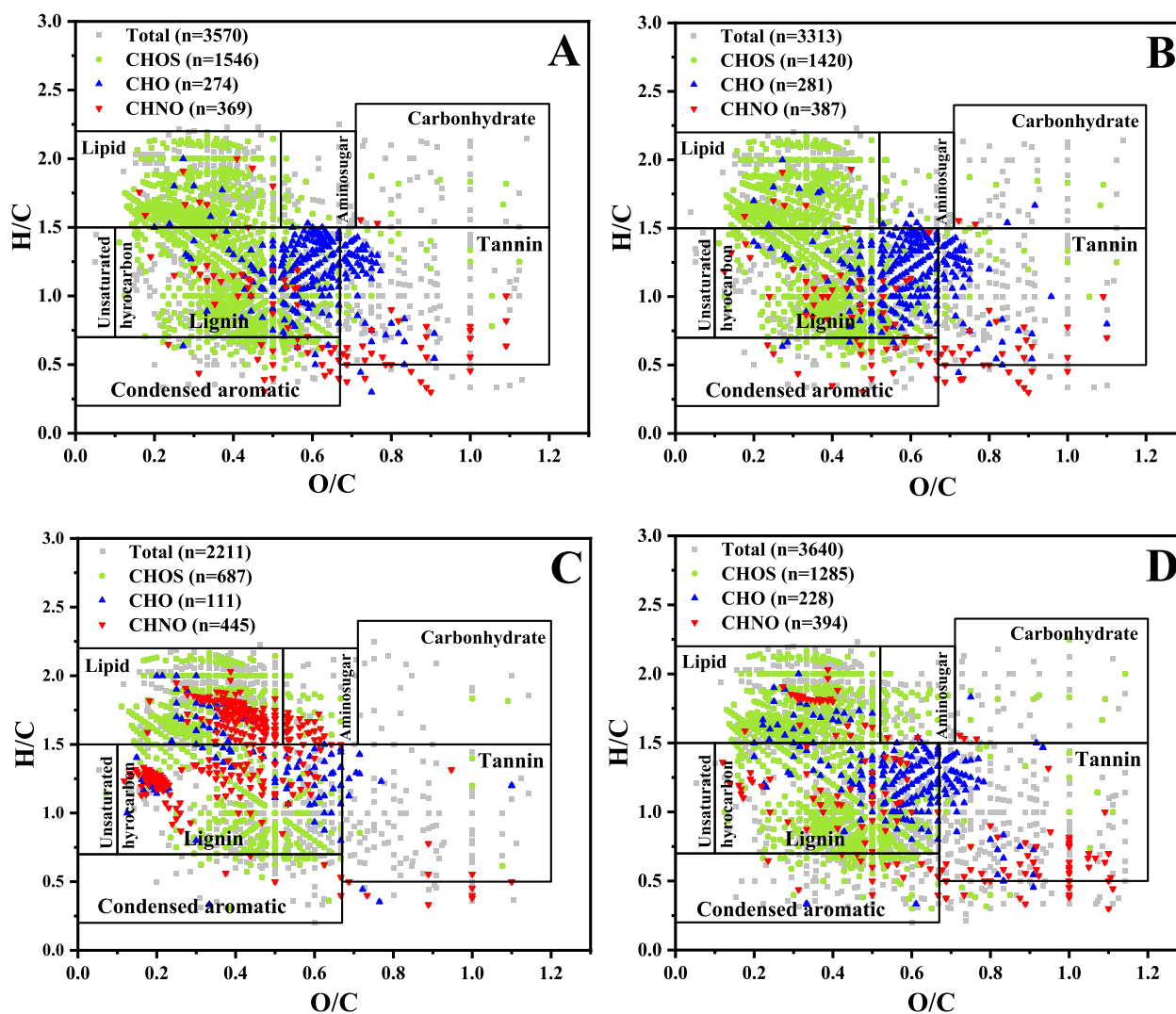
Fig. 6. Chemo-diversity of EPS by FTICR-MS characterization. Circle area corresponds to the relative intensity of each *m/z* ion with CHNO in red and, CHO in blue and CHOS in green. Distribution of molecular formulas of (A) pristine EPS, (B) EPS (pH = 2.5), (C) EPS treated by NaClO and (D) EPS treated by NaClO at pH = 2.5 via Van Krevelen diagrams assignments. (For interpretation of the references to color in this figure legend, the reader is referred to the web version of this article.)

carbonyl derivates of lipid or lignin compounds with aromatic aldehydes/ketones groups (Sun et al., 2018). Specifically, the preliminary proposed molecules of homologous series with DBE = 8 for O_8 was propyl-hydroxyl alkyl ketones structures, and those with DBE = 9 for O_{9-} $_{10}$ were propyl-hydroxyl alkyl ketones and 1-phenyl-1, 3-propanediol dihydroxyphenyl (Fig. 5D) structures, respectively. Moreover, there was also an identified fraction of CHO compounds distributed in the range of $0.67 \leq O/C < 1.2$ and $0.5 < H/C \leq 1.5$, that were generally corresponded to tannins-derived compounds from EPS, that were rich in phenolic hydroxyl and carbonyl groups. Therefore, the lignin, lipids or tannins derived CHO compounds in EPS were probably the important precursors for Cl-DBPs generation during sludge chlorination disinfection process.

3.3.2. Molecular characteristic alteration of EPS and formation of Cl-DBPs

The investigation on the alterations of molecular characteristics of compounds in EPS would help to get insights into the plausible reaction mechanisms between carbonyl derivatives of EPS and NaClO. From Fig. 6C-D, there were no obvious differences in the distributions of CHOS compounds by NaClO treatment in neutrality or acidic conditions. These distributions were still corresponded to lipid or lignin assigned fractions in sludge, implying CHOS compounds were not the main factor for the discrepancy in Cl-DBPs cytotoxicity during neutrality or acidic disinfection conditions. However, as depicted in Figure S6, lignin-

derived carbonyl molecules (CHO, $0.1 \leq O/C < 0.67$, $0.67 < H/C \leq 1.5$) with significant change in that numbers decreased from 2107/1932 to 927/1807 after NaClO treatments at neutrality/ acidic conditions, individually. Meanwhile, NaClO treatment in neutrality environment exhibited higher reaction activity with lipid and lignin-derived compounds in EPS compared to that at acidic environment, which could be attributed to the fact that phenols and alkoxy aromatic rings were easier exposed under alkaline environment caused by hydrolysis of NaClO, and reacted to active chlorine. However, there was an obvious change upon highly oxygenated compounds classes ($0.67 \leq O/C \leq 1.2$, $0.6 < H/C \leq$ 1.5) by NaClO treatment under acidic environment, which were considered as tannin-derived molecules in EPS with abundant phenolic hydroxyl and carboxyl groups (Li et al., 2018; Antony et al., 2014). As depicted in Figure S8, the number of carbonyl molecule in tannin compounds reduced from 241 to 129 after chlorination at neutrality condition, but increased from 229 to 395 after NaClO treatment in acidic environment. It should be noted there were extremely significant changes in the molecular number of N-containing compounds (CHNO), and the number of CHNO molecules increased from 369/387 to 445/394 after NaClO treatment under neutrality/ acidic conditions, respectively. Specifically, CHNO compounds in lipid and lignin assignment fractions increased significantly under neutrality disinfection conditions, whereas the CHO compounds were the major molecules in lignin and tannin

assigned fractions under acidic disinfection conditions. These observations suggested that the lipid, lignin and tannin derived compounds in EPS were transformed into N-containing molecules prior to the Cl-DBPs generation under neutrality disinfection condition. However, the acidic environment could more likely induce the generation of highly oxygenated CHO compounds instead of N-containing compounds during sludge chlorination disinfection, leading to lower Cl-DBPs generation.

To verify the above statement, the alteration of molecular characteristic of the carbonyl and N-containing compounds in the CHO and CHON after NaClO treatment were further analyzed. As illustrated in Fig. 6A and 6C, for the newly produced molecules, lipid and lignin compounds were transformed into N-containing compounds after NaClO treatment in neutrality condition, but they were converted into tannins after NaClO treatment under acidic environment (Fig. 6B and 6D), implying that more N-containing compounds were produced in neutrality chlorination environment. Previous studies reported that N-containing compounds produced from lipid/ lignin were generally rich in phenolic hydroxyl groups and amidogen groups (Qian et al., 2022), which was easily to be replaced by halogens under alkaline condition. During NaClO treatment, it was likely that NaClO addition increased the pH level of sludge system via hydrolysis, and more OH⁻ was produced to facilitate the releasing of N-containing compounds in lignin and lipid fractions. Subsequentially, the generation of Cl-DBPs was increased via nucleophilic substitution between N-compounds and halogens (Cl) under alkaline environment. Therefore, after NaClO treatment, the majority of conversion products of N-compound molecules were distributed in lignin and lipid assignment fractions in a neutral environment, while CHO molecules of lignin and tannin compounds were still the major conversion products in acidic environment.

A more comprehensive comparison of chlorinated compounds showed more molecules were formed in alkaline (n = 37) than that of acidic (n = 19) environment (Fig. 7A-B), and more C_{27}-DBPs was formed in neutrality system, while 2 of 4-Cl-DBPs molecules formed in acidic system. From Fig. 7C-D, plenty identification of Cl-S-DBPs mainly distributed in lignin assigned fractions under both neutrality and acidic disinfection conditions, that was the result of substitution and addition reactions of Cl atoms during NaClO treatment (Figure S9). These reaffirmed that CHO compounds were the main cause of the discrepancy in toxicity of Cl-DBPs instead of CHOS compounds. More specifically, at neutral disinfection condition, the detected Cl-DBPs were assigned to a C_{13}, C_{14}, C_{27} and C_5 backbones that contained between 1 and 3 chlorine atoms, in which C_{27}-DBPs that contains 2 chlorine atoms. However, under acidic condition (pH = 2.5), the detected Cl-DBPs were assigned to a C_5, C_7, C_8 and C_{14} backbones and contained between 1 and 4 chlorine atoms, in which Cl-C_8-DBPs contained 4 chlorine atoms. It should be noted that Cl-C_5-DBPs contained 3 chlorine atoms was generated in both of alkaline and acidic systems, its formula was $C_5HO_3Cl_3$. Besides, the unsaturated of Cl-DBPs in neutral chlorination condition was mainly located in H/C (0.5–1.3) and O/C (0.1–0.6) with only correspondence to the lignin derivatives instead of lipid derivatives (Fig. 7A). However, at acidic environment, Cl-DBPs was mainly located in H/C (0.5–1.3) and O/C (0.5–1.1) that corresponded to tannin
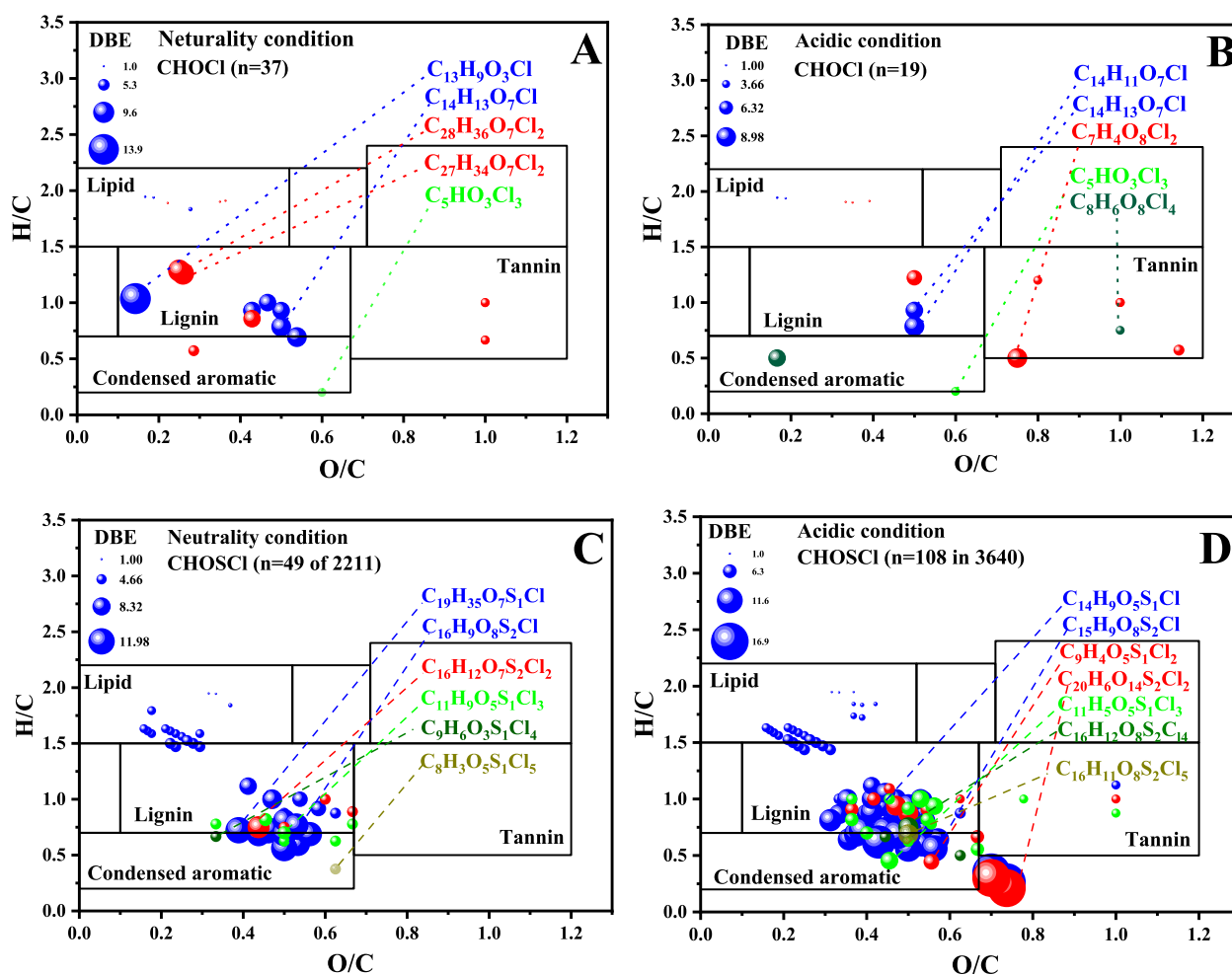

Fig. 7. Cl-DBPs produced during chlorination of EPS and analyzed by FTICR-MS, S-free (A-B) and S-containing (C-D) Cl-DBPs. Molecular formula assignments are based on CHOCl and CHOSCl atoms. Panel A/C and B/D represent Van Krevelen diagrams of produced Cl-DBPs under NaClO treatment at neutrality and acidic conditions, respectively, according to numbers of Cl atom in each assigned formula.
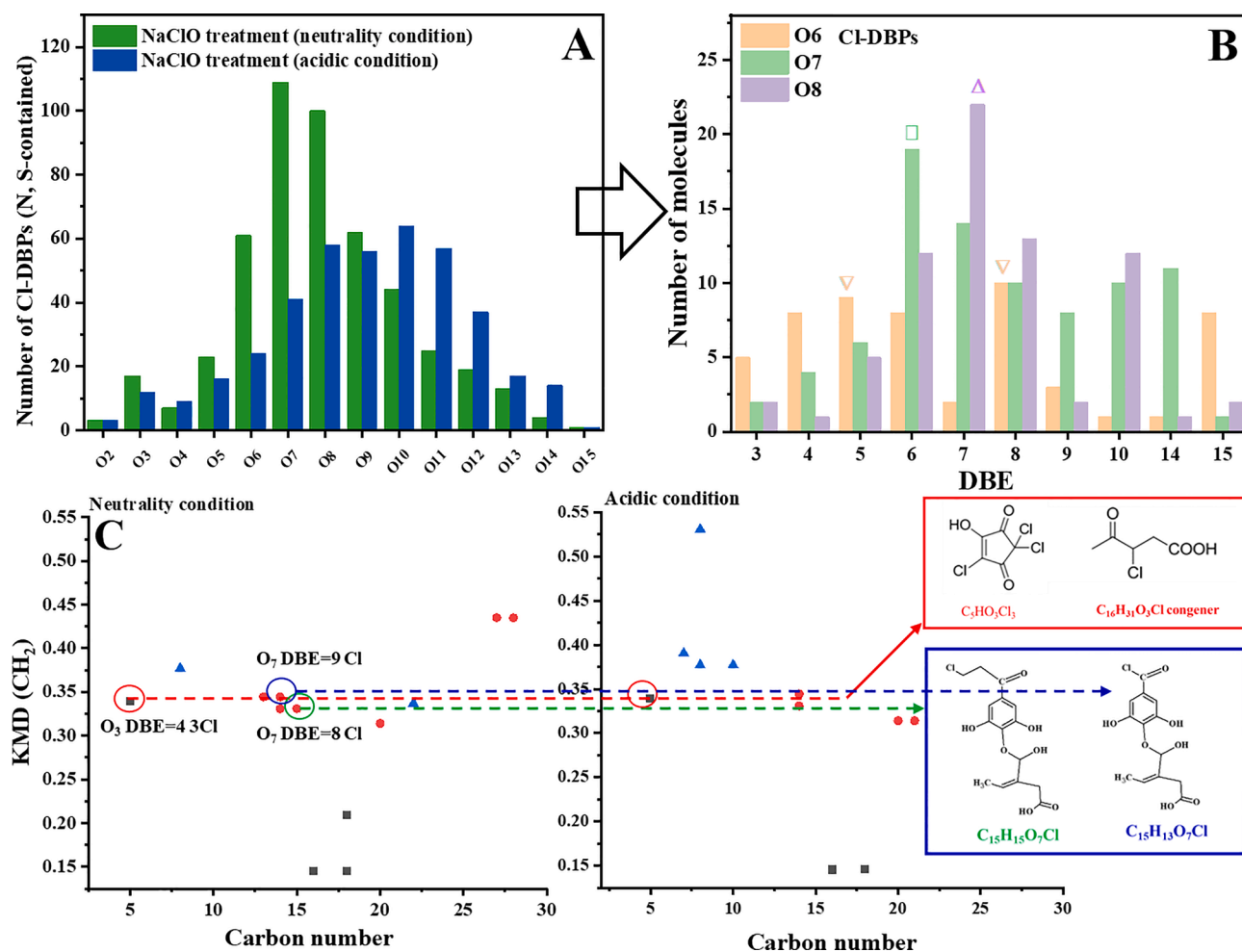
Fig. 8. Molecular characterization of Cl-DBPs after NaClO treatment of EPS solution. (a) distribution of CHO compounds after NaClO treatment by oxygen number; (b) number of Cl-DBP molecules in O_{6-8} species by DBE values; (c) KMD (CH_2)-number of carbon plots of Cl-DBP homologous series and the proposed molecular structures of Cl-DBP.

derivatives (Fig. 7**B**). Combined with the above spectra evidences that the pyrrolic-N, pyridinic-N and protein-N in EPS were the predominant precursors for DBPs generation, and more Cl-DBPs and N-containing compounds produced under neutrality chlorination condition, implying carbonyl-CHO and N-containing compounds representing lignin derivatives mainly contributed to the generation of Cl-DBPs.

3.3.3. Identification of Cl-carbonyl-DBPs

As discussed above, a class of carbonyl Cl-DBPs derived from EPS played the leading role in the sludge cytotoxicity after the NaClO disinfection process. With regard to the carbonyl Cl-DBPs generated during NaClO treatment to EPS, the Van Krevelen and the so-called DBE diagram using oxygen atoms classifying was further applied to separate carbonyl Cl-DBPs compounds and visualize the possible carbonyl Cl-DBPs structure. As illustrated in Fig. 8**A**, after NaClO treatment, a majority of carbonyl compounds was distributed in O_{6-8} series with more than 60 molecules in each species, among which the O_7 species possessed the maximum number of 111 molecules, in which the O atom number decreased from O_{10} to O_7. This result indicated the significant degradation of lignin or tannin compounds into smaller molecules upon NaClO treatment. Moreover, most of O_{6-8} species had high DBE values in the range of 8–22 after NaClO treatment, the DBE values of carbonyl Cl-DBPs increased from 13 to 22 compared to that original molecule in EPS, implying the degree of unsaturation was also increased by chlorination treatment. Besides, more unsaturated carbonyl Cl-DBPs (DBE > 10) with O atom numbers in range of 6–8 were formed after chlorination at

neutrality condition than that at acidic condition (pH 2.5) (Fig. 8**A-B**), which was easily to be taken by cells and showed higher cytotoxicity, evidenced by former results of higher acute toxicity on Q67 lumines bacteria.

In addition, Cl-DBPs molecules with DBE = 8, DBE = 6 and DBE = 7 in O_6, O_7, and O_8 species exhibited the most abundant after NaClO treatment, which was also visualized by the KMD (CH_2)-number of carbon plots with proposed chemical structures in Fig. 8**C**. For instance, the O_7 analogues with DBE = 8 and 9 (i.e., $C_{15}H_{15}O_7Cl$ and $C_{15}H_{13}O_7Cl$) were presented in neutrality condition, but not occurred at acidic environment, indicating that the acidic environment can prevent generation of some Cl-DBPs, especially ones with O ≥ 7 species. Moreover, a analogical skeleton structure of hydroxycyclopentenedione ($C_5H_4O_3$) was observed in sludge treated by NaClO, that has been identified to be trihalo-HCDs (Gong et al., 2005; Pan et al., 2016) during chlorine disinfection system of drinking water. Specifically, the O_3 analogues with DBE = 4 ($C_5HO_3Cl_3$) was formed after NaClO treatment in both neutrality and acidic environments (Fig. 8**C**). This was probably due to the Cl atom replacement of the -H in the $C_5H_4O_3$ molecule, which was also supported by the observation of $[C_5HO_3Cl_3]^+$ in the MS^2 spectra (**Figure S10**) of the O_3 species. Besides, major amounts of compounds were found for Cl-DBPs with higher carbon numbers ≥ 15 at alkaline environment (pH = 8.0), whereas, there was mainly Cl-DBPs with less carbon numbers of < 10 (pH = 2.5) under acidic environment. These results may be indicative for the degradation of larger tannin or lignin compounds into smaller molecules due to the enhancement in oxidation

properties of NaClO at acidic environment. In addition, Cl-DBPs with less carbon numbers was reported hard to form multi-halogenated analogues (Liu et al., 2020), implying the acidic environment can also prevent the formation of multi-halogenated analogues.

Accordingly, the mechanisms of generation of Cl-DBPs can be summarized as follows: lignin, lipids and tannin were released into the sludge bulk solution by NaClO hydrolysis, and created plenty of N-containing compounds via oxidation process by activated chlorine, subsequently the Cl atom reacted with the N-containing compounds to form Cl-DBPs. Meanwhile, it should be noted that N-compounds produced from lignin derivatives contributed to more Cl-DBPs, and alkaline conditions promoted the release and production of N-compounds of lignin derivatives in EPS. However, the acidic environment produced fewer N-compounds neither in lignin nor in tannin derivates in EPS. That is to say, during acidic disinfection conditions, lower toxic Cl-DBPs were generated.

4. Conclusions

In this study, the microorganism *E. Coli* in sludge was found to be effectively inactivated by chlorination disinfection, but a large amount of Cl-DBPs was generated with the addition NaClO to sludge. To control the generation of harmful Cl-DBPs, the mechanisms of EPS transformation and Cl-DBPs generation during sludge chlorination disinfection process were investigated by multispectral analysis in combination with FTICR-MS characterization. As results, concentrations of Cl-DBPs and associated cytotoxicity on Q67 luminous bacterial increased with NaClO dose. During sludge disinfection process, plenty of lignin with $-OCH_3$ groups and N-containing compounds were released due to the alkaline environment caused by NaClO hydrolysis, and a diversity amount of Cl-DBPs with higher DBE values and carbon numbers was formed. These implied that lignin and N-containing compounds in EPS were the major precursors for Cl-DBPs generation. However, under acidic environment, more tannins with $-OH$ groups were released and produced less N-containing compounds, and there was mainly Cl-DBPs with less carbon numbers of < 10 (pH 2.5), causing less multi-halogenated analogues formed. Overall, controlling lignin and N-containing compounds releasing or/ and production was essential to reduce the generation of Cl-DBPs, and acidic environment can prevent the releasing of these compounds, resulted in the reduction of acute toxicity on Q67 luminous bacteria. Therefore, acidification pretreatment was recommended prior to sludge chlorination disinfection in the emergency, and ensure the safety of subsequential disposal for sludge.

Declaration of Competing Interest

The authors declare that they have no known competing financial interests or personal relationships that could have appeared to influence the work reported in this paper.

Data availability

Data will be made available on request.

Appendix A. Supplementary material

Supplementary data to this article can be found online at https://doi.org/10.1016/j.envint.2022.107389.

References

Antony, R., Grannas, A.M., Willoughby, A.S., Sleighter, R.L., Thamban, M., Hatcher, P.G., 2014. Origin and sources of dissolved organic matter in snow on the East Antarctic ice sheet. Environ. Sci. Technol. 48, 6151–6159.

Baluha, D.R., Blough, N.V., Del Vecchio, R., 2013. Selective mass labeling for linking the optical properties of chromophoric dissolved organic matter to structure and composition via ultrahigh resolution electrospray ionization mass spectrometry. Environ. Sci. Technol. 47, 9891–9897.

Bibby, K., Peccia, J., 2013. Identification of Viral Pathogen Diversity in Sewage Sludge by Metagenome Analysis. Environ. Sci. Technol. 47 (4), 1945–1951.

Carrillo-Reyes, J., Barragan-Trinidad, M., Buitron, G., 2021. Surveillance of SARS-CoV-2 in sewage and wastewater treatment plants in Mexico. J. Water Process. Eng. 40, 101815.

Chen, Z., Zhang, W., Wang, D., Ma, T., Bai, R., 2015. Enhancement of activated sludge dewatering performance by combined composite enzymatic lysis and chemical re-flocculation with inorganic coagulants: kinetics of enzymatic reaction and re-flocculation morphology. Water Res. 83, 367–376.

Chen, L., Zhou, H., Yu, B., Huang, Z. W., 2014. Comparison study on hospital wastewater disinfection technology. Adv. Mater. Res. 884-885, 41-45.

Ding, P.F., Song, W.F., Yang, Z.H., Jian, J.Y., 2018. Influence of Zn(II) stress-induction on component variation and sorption performance of extracellular polymeric substances (EPS) from Bacillus vallismortis Bioproc. Biosyst. Eng. 41 (6), 781–791.

Emmanuel, E., Keck, G., Blanchard, J.M., Vermande, P., Perrodin, Y., 2004. Toxicological effects of disinfections using sodium hypochlorite on aquatic organisms and its contribution to AOX formation in hospital wastewater. Environ. Int. 30, 891–900.

EPA, U.S, 2006. National Primary Drinking Water Regulations: Stage 2 Disinfectants and Disinfection Byproducts Rule, p. 388 (Federal Register).

Fu, Q.L., Fujii, M., Watanabe, A., Watanabe, A., Kwon, E., 2022. Formula Assignment Algorithm for Deuterium-Labeled Ultrahigh-Resolution Mass Spectrometry: Implications of the Formation Mechanism of Halogenated Disinfection Byproducts. Anal. Chem. 94 (3), 1717–1725.

Fytili, D., Zabaniotou, A., 2008. Utilization of sewage sludge in EU application of old and new methods-A review. Renew. Sust. Energ. Rev. 12, 116–140.

Gong, H.J., You, Z., Xian, Q.M., Shen, X., Zou, H.X., Huan, F., Xu, X., 2005. Study on the structure and mutagenicity of a new disinfection byproduct in chlorinated drinking water. Environ. Sci. Technol. 39, 7499–7508.

Gonsior, M., Peake, B.M., Cooper, W.T., Podgorski, D., D'Andrilli, J., Cooper, W.J., 2009. Photochemically induced changes in dissolved organic matter identified by ultrahigh resolution fourier transform ion cyclotron resonance mass spectrometry. Environ. Sci. Technol. 43, 698–703.

Gonsior, M., Powers, L.C., Williams, E., Place, A., Chen, F., Ruf, A., Hertkorn, N., Schmitt-Kopplin, P., 2019. The chemodiversity of algal dissolved organic matter from lysed Microcystis aeruginosa cells and its ability to form disinfection by-products during chlorination. Water Res. 155, 300–309.

Gao, Z.-C., Lin, Y.-L., Xu, B., Xia, Y., Hu, C.-Y., Zhang, T.-Y., Qian, H., Cao, T.-C., Gao, N.-Y., 2020. Effect of bromide and iodide on halogenated by-product formation from different organic precursors during UV/chlorine processes. Water Res. 182, 116035.

Gude, V.G., 2015. Energy positive wastewater treatment and sludge management. Edorium J. Waste. Manage. 1, 10–15.

Hall, G.J., Clow, K.E., Kenny, J.E., 2005. Estuarial fingerprinting through multidimensional fluorescence and multivariate analysis. Environ. Sci. Technol. 39, 7560–7567.

Hua, L.-C., Tsia, S.R., Wang, G.-S., Dong, C.-D., Huang, C., 2021. Increasing Bromine in Intracellular Organic Matter of Freshwater Algae Growing in Bromide-Elevated Environments and Its Impacts on Characteristics of DBP Precursors. Environ. Sci. Technol. Lett. 8 (4), 307–312.

He, C.-S., Ding, R.-R., Chen, J.-Q., Li, W.-Q., Li, Q., Mu, Y., 2020. Interactions between nanoscale zero valent iron and extracellular polymeric substances of anaerobic sludge. Water Res. 178, 115817.

Kristiana, I., Gallard, H., Joll, C., Croué, J.P., 2009. The formation of halogen-specific TOX from chlorination and chloramination of natural organic matter isolates. Water Res. 43, 4177–4186.

Lizasoain, A., Tort, L.F.L., García, M., Gillman, L., Alberti, A., Leite, J.P.G., Miagostovich, M.P., Pou, S.A., Cagiao, A., Razsap, A., Huertas, J., Berois, M., Victoria, M., Colina, R., 2018. Human enteric viruses in a wastewater treatment plant: evaluation of activated sludge combined with UV disinfection process reveals different removal performances for viruses with different features. Lett. Appl. Microbiol. 66, 215–221.

Li, X.M., Sun, G.X., Chen, S.C., Fang, Z., Yuan, H.Y., Shi, Q., Zhu, Y.G., 2018. Molecular chemodiversity of dissolved organic matter in paddy soils. Environ. Sci. Technol. 52, 963–971.

Liu, X., Liu, R., Zhu, B., Ruan, T., Jiang, G., 2020. Characterization of Carbonyl Disinfection By-Products During Ozonation, Chlorination, and Chloramination of Dissolved Organic Matters. Environ. Sci. Technol. 54, 2218–2227.

Lavonen, E.E., Gonsior, M., Tranvik, L.J., Schmitt-Kopplin, P., K€ohler, S.J., 2013. Selective chlorination of natural organic matter: identification of previously unknown disinfection byproducts. Environ. Sci. Technol. 47 (5), 2264-2271.

Ningthoujam, R., 2020. COVID 19 can spread through breathing, talking, study estimates. Curr. Med. Res. Pract. 10, 132–133.

Noda, I., Ozaki, Y., 2004. Two-dimensional Correlation Spectroscopy: Applications in Vibrational and Optical Spectroscopy. John Wiley and Sons Inc., London.

Prado, T., Fumian, T.M., Miagostovich, M.P., Gaspar, A.M.C., 2012. Monitoring the hepatitis A virus in urban wastewater from Rio de Janeiro, Brazil. Trans. R. Soc. Trop. Med. Hyg. 106 (2), 104–109.

Pan, Y., Zhang, X.R., 2013. Four groups of new aromatic halogenated disinfection byproducts: Effect of bromide concentration on their formation and speciation in chlorinated drinking water. Environ. Sci. Technol. 47, 1265–1273.

Prasse, C., Ford, B., Nomura, D.K., Sedlak, D.L., 2018. Unexpected transformation of dissolved phenols to toxic dicarbonyls by hydroxyl radicals and UV light. Proc. Natl. Acad. Sci. U.S.A. 115, 2311–2316.

Praspaliauskas, M., Pedisius, N., 2017. A review of sludge characteristics in Lithuania's wastewater treatment plants and perspectives of its usage in thermal processes. Renewable Sustainable Energy Rev. 67, 899–907.

Pan, Y., Li, W.B., Li, A.M., Zhou, Q., Shi, P., Wang, Y., 2016. A new group of disinfection byproducts in drinking water: Trihalo-hydroxycyclopentene-diones. Environ. Sci. Technol. 50, 7344–7352.

Qin, F., Zhao, Y.Y., Zhao, Y.L., Boyd, J.M., Zhou, W.J., Li, X.F., 2010. A toxic disinfection by-product, 2,6-dichloro-1,4-benzoquinone, identified in drinking water. Angew. Chem. Int. Ed. 49, 790–892.

Qian, Y., Chen, Y., Hanigan, D., Shi, Y., Sun, S., Hu, Y., An, D., 2022. pH adjustment improves the removal of disinfection byproduct precursors from sedimentation sludge water. Resour. Conserv. Recycl. 179, 106135.

Rothan, H.A., Byrareddy, S.N., 2020. The epidemiology and pathogenesis of coronavirus disease (COVID-19) outbreak. J. Autoimmun. 109, 102433.

Richardson, S.D., Thruston, A.D., Caughran, T.V., Chen, P.H., Collette, T.W., Floyd, T.L., Schenck, K.M., Lykins, B.W., Sun, G.R., Majetich, G., 1999. Identification of new ozone disinfection byproducts in drinking water. Environ. Sci. Technol. 33, 3368–3377.

Sun, Z.H., Fridrich, B., de Santi, A., Elangovan, S., Barta, K., 2018. Bright side of lignin depolymerization: Toward new platform chemicals. Chem. Rev. 118, 614–678.

Tomlinson, A., Drikas, M., Brookes, J.D., 2016. The role of phytoplankton as precursors for disinfection by-product formation upon chlorination. Water Res. 102, 229–240.

Van Krevelen, D.W., 1950. Graphical-statistical method for the study of structure and reaction processes of coal. Fuel 29, 269–284.

WHO, 2020. WHO Coronavirus Disease (COVID-19) Dashboard | WHO Coronavirus Disease (COVID-19) Dashboard.

Wang, B.B., Liu, X.T., Chen, J.M., Peng, D.C., He, F., 2018. Composition and functional group characterization of extracellular polymeric substances (EPS) in activated sludge: the impacts of polymerization degree of proteinaceous substrates. Water Res. 129, 133–142.

Wang, J., Shen, J., Ye, D., Yan, X., Zhang, Y., Yang, W., Li, X., Wang, J., Zhang, L., Pan, L., 2020. Disinfection technology of hospital wastes and wastewater: Suggestions for disinfection strategy during coronavirus Disease 2019 (COVID-19) pandemic in China. Environ. Pollut. 262, 114665.

Xiao, K., Pei, K., Wang, H., Yu, W., Liang, S., Hu, J., Hou, H., Liu, B., Yang, J., 2018. Citric acid assisted Fenton-like process for enhanced dewaterability of waste activated sludge with in-situ generation of hydrogen peroxide. Water Res. 140, 232–242.

Xie, Q., Liu, N.a., Lin, D., Qu, R., Zhou, Q., Ge, F., 2020. The complexation with proteins in extracellular polymeric substances alleviates the toxicity of Cd (II) to Chlorella vulgaris. Environ. Pollut. 263, 114102.

Ma, M., Zhao, W., Liu, H., 2010. Application progress of hospital wastewater treatment methods. Occup. Health 26, 1180–1182.

Yu, J.L., Li, Q., Yan, S.C., 2013. Design and running for a hospital wastewater treatment project. Adv. Mater. Res. 777, 356–359.

Yin, C., Meng, F., Chen, G.H., 2015. Spectroscopic characterization of extracellular polymeric substances from a mixed culture dominated by ammonia-oxidizing bacteria. Water Res. 68, 740–749.

Yuan, Z.W., He, C., Shi, Q., Xu, C.M., Li, Z.S., Wang, C.Z., Zhao, H.Z., Ni, J.R., 2017. Molecular insights into the transformation of dissolved organic matter in landfill leachate concentrate during biodegradation and coagulation processes using ESI FT-ICR MS. Environ. Sci. Technol. 51, 8110–8118.

Zhang, X., Minear, R.A., 2002. Characterization of high molecular weight disinfection byproducts resulting from chlorination of aquatic humic Substances. Environ. Sci. Technol. 36 (19), 4033–4038.

Zhang, T.-Y., Lin, Y.-L., Xu, B., Cheng, T., Xia, S.-J., Chu, W.-H., Gao, N.-Y., 2016. Formation of organic chloramines during chlor(am)ination and UV/chlor(am) ination of algae organic matter in drinking water. Water Res. 103, 189–196.

Zhai, H.Y., Zhang, X.R., Zhu, X.H., Liu, J.Q., Ji, M., 2014. Formation of brominated disinfection byproducts during chloramination of drinking water: New polar species and overall kinetics. Environ. Sci. Technol. 48, 2579–2588.

Zhao, Z., Gonsior, M., Luek, J., Timko, S., Ianiri, H., Hertkorn, N., Schmitt-Kopplin, P., Fang, X., Zeng, Q., Jiao, N., Chen, F., 2017. Picocyanobacteria and deep-ocean fluorescent dissolved organic matter share similar optical properties. Nat. Commun. 8, 15284.

Zhu, X., Yang, S., Wang, L., Liu, Y., Qian, F., Yao, W., Zhang, S., Chen, J., 2016. Tracking the conversion of nitrogen during pyrolysis of antibiotic mycelial fermentation residues using XPS and TG-FTIR-MS technology. Environ. Pollut. 211, 20–27.